Dynamic Evacuation Path Planning for Multi-Exit Building Fire: Bi-Objective Model and Algorithm

Wenling Guan, Shuai Hou, Gangjie Yu and Haofeng Gong, School of Environmental Science and Safety Engineering, Tianjin University of Technology, 391 Binshui Xidao, Xiqing District, Tianjin 300384, China

Siqi Guan, Tianjin Fire Research Institute of Ministry of Emergency Management, Tianjin 300381, China

Junying Zhao ⑩*, School of Environmental Science and Safety Engineering, Tianjin University of Technology, 391 Binshui Xidao, Xiqing District, Tianjin 300384, China

Abstract. Building fires are one of the most common fire types and tend to cause heavy casualties. During the evacuation, the shortest path makes the escapees leave the accident scene faster. Meanwhile, the safety of escapees in the evacuation process cannot be ignored. Optimal path should both ensure evacuation efficiency and maximize the safety of escapees. A bi-objective path planning model, which considers both path risk and path length, is presented. Path risk is based on five risk factors that are likely to cause casualties in a fire: carbon monoxide (CO), hydrogen cyanide (HCN), temperature, visibility, and crowding. The linear weighted sum method is used to convert the risk-objective model and the length-objective model into a dynamic bi-objective path planning model. The Dijkstra algorithm is modified to solve the model. The modified algorithm outperforms the traditional Dijkstra algorithm in terms of both efficiency and adjustment ability. The simulation analysis of a building fire shows that the bi-objective model and algorithm can plan a combined optimal evacuation path for escapees considering risk and path length, which avoids the area with high risk level and optimizes the evacuation path length.

1. Introduction

The fire situation in China has undergone remarkable changes with rapid economic growth in recent years [1]. Buildings with complex structure, such as stadiums and shopping malls, began to proliferate to meet the needs of consumers.

---

*Correspondence should be addressed to: Junying Zhao, E-mail: zhao_jy2@163.com

Wenling Guan and Gangjie Yu have contributed equally to this work and also co-first authors.

Meanwhile, the frequent occurrence of building fire has caused serious mass disasters. For example, a fire occurred in Jilin Shopping Mall on November 5, 2010 with a death toll of 19 [2] and Anyang Trade Company fire happened in November 21, 2022 with a death toll of 38. Statistics from the Fire and Rescue Department Ministry of Emergency Management showed that 168 people have died in building fires in China in 2021. Asphyxiating and irritating gases generated in building fires threaten the safety of evacuees, and those who successfully escape but have been exposed to high temperatures and concentrations of hazardous gases also face the possibility of death even after the fire has ended [3]. Therefore, emergency evacuation should focus not only on improving evacuation efficiency and shortening evacuation time but also minimizing the risks that evacuees may suffer in the process of evacuation.

Evacuation of pedestrians is a process of path decision and moving to the emergency exit when threatened. Conventional static path indication signs guide pedestrians to escape in unfamiliar environments, but static signs fail to predict the risks that people may encounter in escape paths. Therefore, researchers have paid considerable attention to the field of evacuation path optimization in recent years. Many studies have focused on optimizing evacuation time or path length to ensure the safety of evacuees from the perspective of evacuation efficiency [4–13] but ignore the potential risks caused by the spread of fire to different paths. Some scholars have used fire risk as the optimization objective. Balboa et al. [14] proposed a pathway to prohibit excessive hazardous gases and avoid the risk of hazardous gases in fires. Wang et al. [15] put forward an optimization objective that minimizes the total amount of harmful gas inhalation. Faouzi Kamouna [16] considered the concentration of harmful gases, temperature, and crowding in the path. Wang et al. [17] took into account the influence of smoke temperature, visibility, and CO concentration on evacuation in drilling platforms. In addition to considering the risk of combustion product in fire, many studies have emphasized evacuation models that integrate fire risk with other influencing factors. Chu et al. [18] established a model for optimizing variable pedestrian evacuation guidance that considers congestion, hazard, and compliance behavior. Mirahadi and McCabe [19] used evacuation time, proximity of evacuation path to the fire location, crowding, and next expected isolation of the fire area (unpassable areas) as optimization objectives. Song et al. [20] proposed an evacuation route selection approach that considers hazards and time for indoor spaces and assessed fire hazard using the fractional effective dose of carbon monoxide, oxygen, and carbon dioxide and heat.

Although these studies have introduced path risk into the path planning model, the selection of path risk factors presents limitations. Faouzi Kamouna [16] and Song et al. [20] neglected visibility. Risk factors proposed by Wang et al. [17] failed to consider the harm caused by heat. On the basis of previous studies, this work optimized risk factors, including smoke toxicity, temperature, visibility, and crowding. However, the risk classification standard is unclear. Song et al. [20] assessed the fire risk through the fractional effective dose although this method is not applicable to the evaluation of crowding. Shi et al. [21] assessed risk in fire evacuations from several aspects but the calculation of risk levels lacks homoge-

nization. A semiquantitative method is cited in this study to homogenize the risk characterization and classify the different degrees of potential harm to personnel.

Researchers have proposed various methods for solving the path planning problem and achieving the optimization objective. A* [22] is a widely used heuristic-based algorithm that has been successfully used to solve the shortest path problem and obtain the optimal path for various path planning problems. However, it does not apply to path planning of multiple exits. Evolutionary computing (EC) methods, such as genetic algorithm (GA) [23], particle swarm optimization (PSO) [24], ant colony optimization (ACO) [21], and artificial bee colony (ABC) [25], have been gradually introduced into path planning in recent years. Meanwhile, the modification of these methods and integration of different algorithms have rapidly developed [26] despite demonstrating some drawbacks. For instance, GA typically converges prematurely to the local optimal solution, and its ability to explore space is limited. PSO depends on users to adjust the control parameters and achieve the required solution. In addition, premature convergence also exists in the evolution process when PSO is used to deal with complex problems. Premature convergence is not ideal because the result is only locally optimal instead of being globally optimal. The typical occurrence of premature and stagnation phenomena in ant colony algorithms when the swarm scale is large imposes restrictions on further applications [25]. Dijkstra algorithm is a simple but powerful classical method that has been widely used in various fields for path selection and solving single-objective shortest path problems in static networks [27–32]. However, the Dijkstra algorithm is unsuitable for solving shortest path problems in dynamic networks as well as the multi-exit path planning problem. The modified Dijkstra algorithm utilized in solving the bi-objective model proposed in this study can be applied to the calculation in dynamic networks. This extended algorithm significantly optimizes the solution efficiency of the model in multi-exit building fires and solves the bi-objective model to find a comprehensive optimal solution with dynamic adjustability that traditional algorithms lack.

A bi-objective model that considers path risk and length is proposed in this study. The risks considered in the model are more comprehensive than those of previous studies because they take into account hazardous gases, temperature, visibility, and crowding. A semiquantitative risk classification standard is adopted to characterize the risk in a more homogeneous manner. The Dijkstra algorithm is optimized to differentiate it from the classical version in the following aspects: dynamic adjustability, path disabling, and efficiency. The model and algorithm in this study will contribute to solving the multi-exit fire evacuation problem by planning a safe and efficient evacuation path for escapees.

2. Path Planning Models

2.1. Building Emergency Evacuation Network

Path selection is a multi-objective optimization problem that must weigh many factors during evacuation. Intricate passages within the building form a connected network graph on the basis of graph theory. The passage is regarded as the arcs,

the intersections of the passage are the nodes, and the arcs represent the connections between nodes of the network. A building with fifteen rooms and two exits will be taken as the objective of the study, and its emergency evacuation network is shown in Figure 1.

The emergency evacuation network is defined as an undirected graph $G(V, E)$, as shown in Figure 1, where V is the set of nodes and E is the set of arcs, and $v_1, v_2, \ldots v_n$ is set as the nodes in the network, that is, $V = \{v_1, v_2, \ldots v_n\}$. v_n is the destination node, v_s is the source node, and e_{ij} is the physical length of (v_i, v_j).

The two optimization objectives herein are path risk level and length. The optimal evacuation path refers to the path that encompasses the risk level as low as possible and the length as short as possible. The bi-objective optimization model can be formulated as follows:

$$F_1 = minf_1 \tag{1}$$

$$F_2 = minf_2 \tag{2}$$

in which f_1 represents the risk level in the evacuation path, F_1 is the minimum risk level among all evacuation paths. f_2 is the physical length of the evacuation path, and F_2 is the minimum physical length in all evacuation paths.

2.2. Risk-Objective Model

2.2.1. Establishment of the Model The principle of the risk-objective model is to prioritize the safety of evacuees, with the goal o1f mitigating potential harm to evacuees during the evacuation. The following additional notation is used.

(1) R_{ij}: The risk level of arc (v_i, v_j).
(2) x_{ij}: The decision variable with $x_{ij} = 1$ if arc (v_i, v_j) is included in the fixed path and 0 otherwise.

The formulation of the risk-objective model under the real-time development of fire is described as follows:

Model I:

$$F_1 = \min f_1 = \sum_{i=s}^{n} \sum_{j=s}^{n} x_{ij} R_{ij} \tag{3}$$

S.t.

$$\sum_{\substack{j=s \\ j \neq i}}^{n} x_{ij} - \sum_{\substack{j=s \\ j \neq i}}^{n} x_{ji} = \begin{cases} 1 & i = s \\ -1 & \\ & i = n \\ 0 & otherwise \end{cases} \tag{4}$$
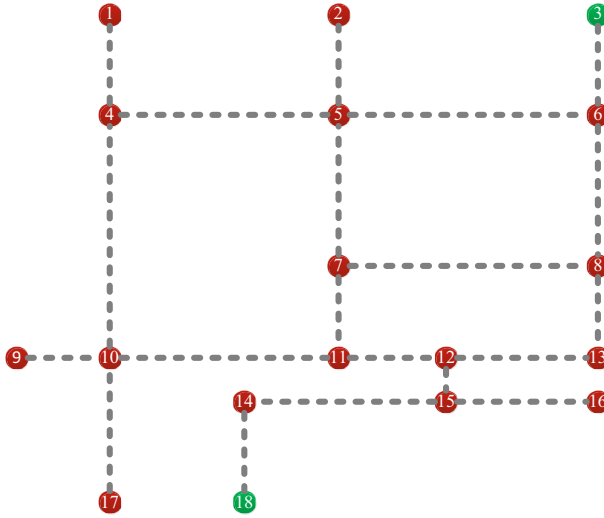
Figure 1. Emergency evacuation network structure.

$$\sum_{\substack{j=s \\ j \neq i}}^{n} x_{ij} = \begin{cases} \leq 1 & i \neq n \\ = -1 & i = n \end{cases} \tag{5}$$

$$x_{ij} = 0, 1, \, i = 1, 2, \ldots, n, \, j = 1, 2, \ldots, n \tag{6}$$

where Eq. (3) represents the objective of model, which minimizes the risk level along the path. Constraint (4) guarantees a feasible path from source node v_s to destination node v_n by restricting the value of x_{ij}. Considering the feasibility of the evacuation plan and the urgency of the evacuation time, Constraint (5) is used to ensure that there are no paths with loops [33]. Constraint (6) is the 0–1 integer constraint of the decision variable x_{ij}.

2.2.2. Characterization of R_{ij} Any fire risk that causes physical and psychological damage to evacuees increases the possibility of death. Asphyxiating gases, such as carbon monoxide (CO) and hydrogen cyanide (HCN), and high temperatures are the main causes of death during and after fires [3]. Smoke output from a fire can reduce visible distance and delay escape time as it spreads out in the path [34]. Overcrowding also increases the stay time of evacuees at the fire scene. Huo et al. [35] studied the effect of pedestrian density on evacuation results and showed that the greater the pedestrian density, the more the pedestrians fall to the ground and die. Therefore, we use risk factors, including CO concentration, HCN concentration, temperature, visibility, and crowding, in calculating the path risk level.

R_{ij} is the weighted average and expressed as follows:

$$R_{ij} = \alpha_1 r_{ij}^{CO} + \alpha_2 r_{ij}^{HCN} + \alpha_3 r_{ij}^{T} + \alpha_4 r_{ij}^{Vis} + \alpha_5 r_{ij}^{D} \tag{7}$$

where the sum of weight coefficients $\alpha_i \in [0,1]$ is 1. These coefficients denote the weights of different risk factors. The risk index is defined as the value converted from real-time changes of risk factors in arc (v_i, v_j). $r_{ij}^{X} \in [0,1]$ corresponds to the risk index associated with CO, HCN, temperature, visibility, and crowding.

A semiquantitative method is cited to homogenize the risk characterization and classify the different degrees of potential harm to personnel from risk factors [16]. Risk classification are listed in Table 1.

(1) r_{ij}^{CO} and r_{ij}^{HCN}

Acute exposure guideline levels (AEGLs) represent threshold exposure limits (adverse health effects are likely to occur beyond this level) for the general public and are applicable to emergency exposures ranging from 10 min to 8 h [36]. Three levels, namely, AEGL-1, AEGL-2, and AEGL-3, were developed and differentiated for five exposure periods (10 min, 30 min, 1 h, 4 h, and 8 h) using various degrees of toxic effects. AEGLs refer to airborne concentrations of chemicals above which a person could experience evident discomfort or irritation (AEGL-1), serious and long-lasting health effects (AEGL-2), and life-threatening effects or death (AEGL-3). AEGLs with exposure times of 10 and 30 min were selected as the risk index of CO and HCN [36, 37]. According to Table 1, ranges for CO levels are converted into risk indexes [16] (Table 2).

Similarly, ranges for HCN levels are converted into risk indexes on the basis of AEGLs at exposure times of 10 and 30 min of HCN (Table 3).

(2) r_{ij}^{T}

Human tolerance to high temperature is limited. The maximum tolerance time ($\tau(T)$) as a function of temperature can be summarized as Eq. (8) [21]. The results are listed in Table 4.

$$\tau(T) = 1812e^{-0.046T} \tag{8}$$

High temperatures indicate a short tolerance time of humans. The tolerance time of a human is only 7 min at 120 °C. Hence, the maximum tolerance time of 7 min is defined as the highest risk classification.

Ranges for temperature levels are converted into the risk index r_{ij}^{T} on the basis of the calculated maximum tolerance time at different temperatures (Table 5).

(3) r_{ij}^{Vis}

The risk classification criteria of visibility are based on the experimental data of British subjects [38]. r_{ij}^{Vis} is determined according to the visible distance when evac-

Table 1
Risk Classification and Risk Index

Risk Classification	Risk Index
I	0
II	0.5
III	0.7
IV	1

Table 2
Classification of r_{ij}^{CO}

CO(ppm)	Risk Classification	r_{ij}^{CO}
CO < 150	I	0
$150 \leq CO < 420$	II	0.5
$420 \leq CO < 600$	III	0.7
$CO \geq 600$	IV	1

Table 3
Classification of r_{ij}^{HCN}

HCN (ppm)	Risk Classification	r_{ij}^{HCN}
HCN < 10	I	0
$10 \leq HCN < 17$	II	0.5
$17 \leq HCN < 21$	III	0.7
$HCN \geq 21$	IV	1

Table 4
Maximum Human Tolerance Time at Different Temperatures

Temperature/°C	40	60	80	100	120
Time/min	290	115	46	20	7

uees choose to turn. The experimental results demonstrated that 100% of experimenters choose to change direction when the visible distance of the passage is less than 0.6 m; therefore, the visible distance of 0.6 m is defined as the highest risk classification. Only 9% of experimenters chose to change direction when the visible distance of the passage is greater than 3.7 m; hence, the visible distance of

Table 5
Classification of r_{ij}^T

temperature T(°C)	Risk Classification	r_{ij}^T
T < 60	I	0
60 ≤ T < 80	II	0.5
80 ≤ T < 120	III	0.7
T ≥ 120	IV	1

Table 6
Classification of r_{ij}^{Vis}

Visible Distance (m)	Risk Classification	r_{ij}^{Vis}
Vis > 3.7	I	0
1.8 < Vis ≤ 3.7	II	0.5
0.6 < Vis ≤ 1.8	III	0.7
Vis ≤ 0.6	IV	1

3.7 m is set as the acceptable risk. Visible distance values converted into the risk index r_{ij}^{Vis} are presented in Table 6.

(4) r_{ij}^D

Crowding exerts a significant effect on the evacuation time because it determines the walking speed of evacuees. Interpersonal walking contact and stagnation occur when the crowd density reaches 4 person/m^2 [39]; therefore, the crowd density of 4 person/m^2 is defined as the highest risk classification. Evacuees can walk freely without contact when the crowd density is below 1.8 person/m^2; thus, 1.8 person/m^2 is defined as the acceptable risk. Ranges for density levels converted to the risk index are listed in Table 7.

2.3. Length-Objective Model

In addition to risks in the emergency evacuation path, the length of the path is a key factor that must be considered. Although the chosen evacuation path is low risk in some cases, it requires a large number of detours. Related studies have shown that crowding typically happen at the intersections of two arcs in the emergency network [33]. Meanwhile, an excessively long evacuation path will also inevitably affect the evacuation time, thereby increasing the probability of suffering from risks. On the basis of the risk-objective model proposed in Sect. 2.1, a length-objective model is established with the aim of minimizing the length of evacuation paths.

The formulation of the length-objective model is as follows:
Model II:

Table 7
Classification of r_{ij}^D

Crowd Density (person/m^2)	Risk Classification	r_{ij}^D
D < 1.8	I	0
1.8 ≤ D < 3	II	0.5
3 ≤ D < 4	III	0.7
D ≥ 4	IV	1

$$F_2 = \min f_2 = \sum_{i=s}^{n} \sum_{j=s}^{n} x_{ij} e_{ij} \tag{9}$$

S.t.

  (4), (5) and (6)

2.3.1. Bi-objective Model Models I and II can be planned for the evacuation path with the minimum risk level and the evacuation path with the minimum length, respectively. However, this section establishes a bi-objective path planning model on the basis of Models and II to obtain the integrated optimal evacuation path with respect to fire risk and path length as well as the Pareto optimal solution of the two objective functions.

  A bi-objective optimization problem will involve multiple objective functions and constraints. The other objective may deteriorate when one objective reaches optimality. Obtaining the optimal solution for all objectives is difficult in the case of mutual constraints and interactions of objective functions. Different levels of attention should be given to each optimization objective, especially when the risk level in the path is excessively high, and the weight of the risk in the objective function should be increased. Moreover, the value of the optimized objective function corresponding to a specific Pareto optimal solution will likely fail to meet the actual needs of evacuees. Multiple Pareto solutions can be determined on the basis of the Dijkstra algorithm, and the results can be dynamically adjusted as the fire spreads. Linearly weighing the optimization objectives is a common method for solving the bi-objective optimal path [21]. Each weight represents the relative importance of each objective to some extent.

  We use the linear weighted sum method to convert the risk and length-objective models into a bi-objective path selection model as shown below:

$$F = \gamma_1 \frac{f_1}{f_1^*} + \gamma_2 \frac{f_2}{f_2^*} \tag{10}$$

S.t.

  (3), (4), (5), (6) and (9)in which $\gamma_1 \geq 0, \gamma_2 \geq 0$, and $\gamma_1 + \gamma_2 = 1$. f_1^* denotes the ideal risk level in the evacuation path, representing the minimum risk level from v_s

to v_n; f_2^* denotes the ideal path length in the evacuation path, representing the shortest length from v_s to v_n. If the objective weight vectors γ_1 and γ_2 vary, monotonic decreases and increases occur in f_1 and f_2, respectively.

3. Modified Dijkstra Algorithm

3.1. Main Part and Calling Algorithm

The classical Dijkstra algorithm is modified to solve the dynamic bi-objective model. The main part of the newly modified algorithm is shown in Figure 2, and algorithm b is the calling algorithm of the main part. The problem is reduced to using $\gamma_1 = 0$ or $\gamma_2 = 0$ to ensure that Algorithm b can be applied directly when solving the single objective problem. However, if a bi-objective is to be solved, then the optimal path will be constructed at the end of algorithm b through the search space of the weight vector in Figure 2. The essential idea of the calling algorithm b is that each additional subsequent node will update the weights of the network on the basis of the path that was found when implementing the Dijkstra algorithm [40]. The following notations are used to express the main part of the algorithm (see Figure 2) and the calling algorithm (see Algorithm b).

Let $p(v_j)$ be the minimum value of objective function F among the evacuation paths. B_j represents the path with F equal $p(v_j)$; S is the set of nodes for which the shortest path has been found; δ represents the optimal point; $f_1(\delta)$ and $f_2(\delta)$ represent the values of f_1 and f_2 in the path of $F = p(v_j)$, respectively; K denotes the number of arcs in the selected path; r^* denotes a set criterion that represents the upper limit of the ideal risk level, that is, humans will likely suffer from the threat of fire beyond this point; and r^* is set to 0.7.

Algorithm b

3.2. Risk Threshold

The risk threshold is imposed on each arc. If a risk factor of the objective node reaches the risk threshold when the algorithm searches for the path with the minimum objective value F, then the algorithm will ignore this node and search again for the path with the minimum objective value F. The node with crowding reaches the risk threshold and the four other risk factors that fail to reach the risk threshold will be reconsidered when all paths that can be selected are unavailable. These risk thresholds can be determined on the basis of the results of the analysis in 2.1, where the value of a risk index reaching 1 is set as the risk threshold. Therefore, the risk threshold is 600 ppm for CO, 21 ppm for HCN, 120 °C for temperature, 0.6 m for visible distance, and 4 persons/m^2 for crowded density.

3.3. Super-Destination Node

Several exits exist in the majority of modern buildings, and the evacuation problem can be solved in an emergency evacuation network with multiple destination nodes. The emergency evacuation network in Figure 1 shows the problem of multiple destination with source nodes. The classical Dijkstra algorithm requires two
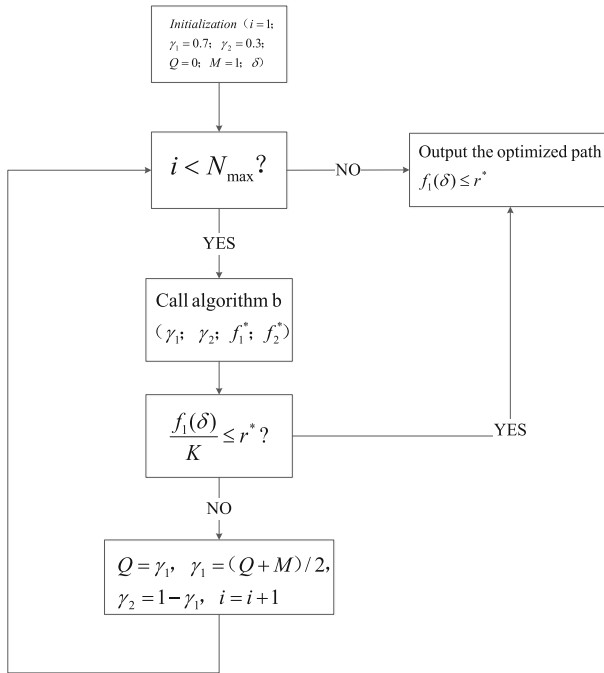
Figure 2. The main part of the modified algorithm.

exits (v_3 and v_{18}) as destination nodes and others as source nodes. The algorithm must be repeatedly and inefficiently called 16 times to solve the model. Note that demanding high efficiency in solving the algorithm is logical considering the urgency of evacuation.

The modified algorithm establishes a super-destination node [41], which connects all exits to change the original network structure and sets the weights of edges connecting each exit to the super-destination node to zero. Moreover, it transforms super destination node into a source node and transforms each source node into a destination node. Therefore, the optimal path from the super-destination node to other nodes can be solved by calling the Dijkstra algorithm only once and then converting the original problem into a single source node and single destination node problem. This method does not affect the final result and significantly improves the efficiency of the solution. The structure of the changed network is shown in Figure 3.

4. Case Study

A simulation experiment of a building fire is used in this section to demonstrate the reliability and feasibility of the bi-objective model and modified Dijkstra algorithm.
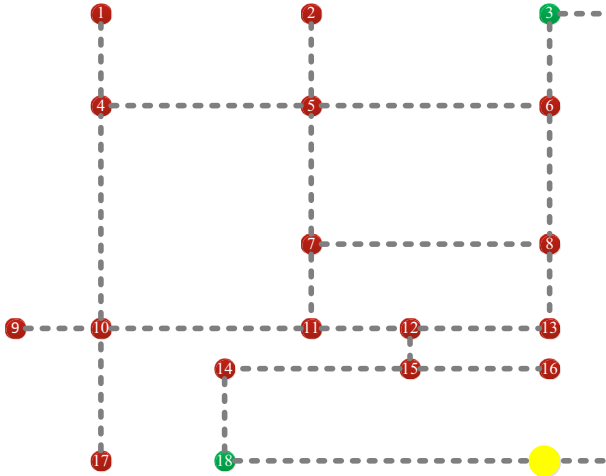
**Figure 3. The structure of the modified emergency network.**

4.1. *Introduction of Simulation Scenario and Risk Factor Weight*

The simulation experiment is based on a building with fifteen rooms, two exits (Exits A and B), and a total area of 1640 m². The emergency evacuation network is shown in Figure 1. A 3D model of the building is built using PyroSim software, and internal channels are evenly arranged with CO detectors, HCN detectors, visibility detectors, temperature detectors, and thermocouples. The initial temperature was set to 20 °C. The sofa rest area in the corner was selected as the fire point.

The worst-case scenario considered in the experiment assumes that the sprinkler system fails and the combustion surface is set to sustainable combustion. The HRR (heat release rate) is the product of the fire area and HRRPUA (heat release rate per unit area). HRRPUA is set to 2000 KW/m² and the burning area of the fire source is set to 0.45 m² in the PyroSim model; hence, HRR is equal to 900 KW. The completed 3D PyroSim model is shown in Figure 4.

The numerical simulation of fire was carried out after building the model. Data of 30-, 90-, and 200-s moments were used in the analysis. The fire development process can be seen through a 3D smoke dispersion simulation and CO, HCN, visibility, and temperature slices. The CO slice is taken as an example. Fire conditions at 30-, 90-, and 200-s moments were obtained through the 3D smoke dispersion simulation (Figure 5).

Weight coefficients of five risk factors in this experiment are set according to the statistical data of fire death causes. Asphyxiating gases, especially CO, are the most lethal risk factor in case of fire. Although inhalation of HCN may lead to rapid incapacitation, its effects are smaller than those of CO in many cases. For instance, fires that produce cyanide give off CO and combustion conditions producing high yields of HCN also lead to high yields of CO [3]. CO is generally a more lethal risk factor in building fires compared with HCN; therefore, the weight of asphyxiating gases, especially CO is set higher in this case, with temperatures
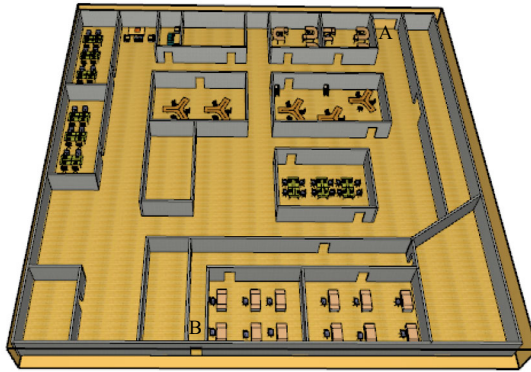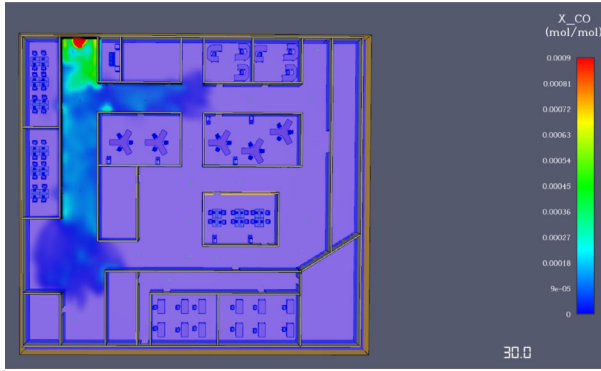
(a) Frontal top view perspective of the model
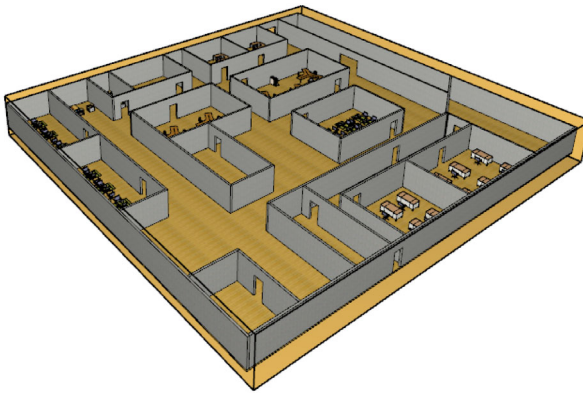
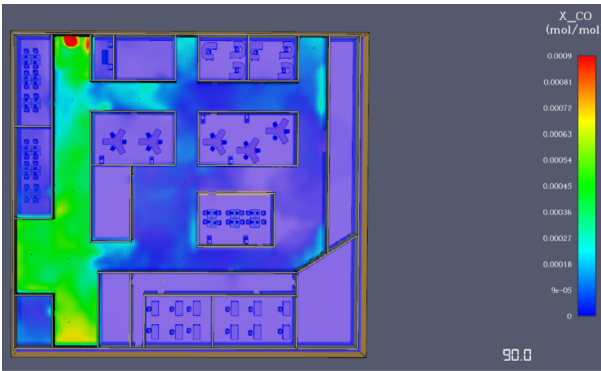(b) Side top view perspective of the model
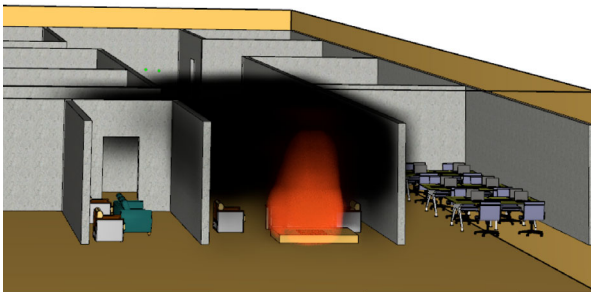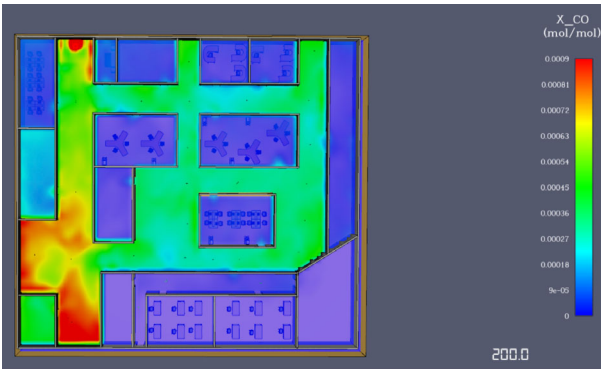

(c) The location of the fire

Figure 4.   PyroSim 3D model.

(a) 30s

(b) 60s

(c) 200s

Figure 5.   3D smoke dispersion and CO slice.

being second only to both. Visibility and crowding affect the speed of people but could not this cause crowd crash, which in turn causes death; thus, the weight of visibility and crowding is typically minimized. Weight coefficients of the five risk indexes in this case were finally set to $\alpha_1 = 0.4, \alpha_2 = 0.3$, $\alpha_3 = 0.2, \alpha_4 = 0.05,$ and $\alpha_5 = 0.05$.

4.2. Simulation Results and Analysis

Data of visibility, CO concentration, HCN concentration, and temperature in each path can be obtained through the detectors in the channel. Crowd density is set randomly via MATLAB. Fire data and crowd density of each path at 30, 90, and 200 s are listed in Tables 8, 9, and 10, respectively.

The bi-objective path planning model and algorithm are programmed using MATLAB, and optimal evacuation paths of different nodes at various moments and their objective value F are generated by combining fire data within each segment of the path obtained from the PyroSim simulation and the set crowding data. Node 7 is used as an example to analyze the optimal evacuation paths of people in this position at 30, 90, and 200 s. The optimal evacuation path is marked in green and the path where the risk factor reaches the risk threshold is marked in orange. The results of the optimal evacuation path for node 7 are shown in Figure 6.

The smoke does not spread widely when the fire lasts for 30 s. The optimal evacuation path at this time is determined via path crowding and length. Paths v_5–v_7 and v_{12}–v_{15} will be ignored by the algorithm because they reach the risk threshold at 30 s. Finally, the optimal evacuation path of node 7 is determined as v_7—v_8—v_6—v_3. The optimal evacuation path is the evacuation path with the minimum path length of 34.7 m and objective value F of 0.035. The smoke spreads nearly throughout the building when the fire occurs for 90 s, but other paths, except for v_1—v_4, v_4—v_{10}, v_9—v_{10}, and v_{10}—v_{17}, fail to reach the risk threshold. The optimal evacuation path at this time is mainly determined on the basis of the risk level. The optimal evacuation path for node 7 at 90 s is determined as v_7—v_{11}—v_{12}—v_{15}—v_{14}—v_{18}, with an evacuation path length of 42.3 m and objective value F of 0.042. The majority of paths have reached the risk threshold when the fire occurs for 90 s due to the prolonged diffusion of smoke. The algorithm will resume the forbidden paths and retraverse them to obtain the path with the minimum objective value F because paths of the nodes are generally infeasible. The optimal evacuation path for node 7 at 200 s is still determined as v_7—v_{11}—v_{12}—v_{15}—v_{14}—v_{18}, with an evacuation path length of 42.3 m and objective value F of 1.302. The optimal evacuation path for node 7 is summarized in Table 11. Combined with the fire numerical simulation results of PyroSim and smoke dispersion simulation, the optimal evacuation path is obtained through the path planning model and algorithm by avoiding the area with high risk level and optimizing the evacuation path length. If the classical shortest path algorithm is used, then the path chosen will always be v_7—v_8—v_6—v_3 or v_7—v_5—v_6—v_3. However, this approach has failed to provide safe path for escapees as the fire progresses Figure 7.

Table 8
Fire Data and Crowd Density for Each Path at 30 s of fire

Path	Visibility (m)	CO (ppm)	HCN (ppm)	Temperature (°C)	Crowd Density (person/m^2)
v_1—v_4	1.808	208	12	35.709	1.403
v_4—v_5	2.166	170	12	33.23	2.600
v_4—v_{10}	2.034	182	13	33.55	0.309
v_2—v_5	30	0	0	20.524	1.452
v_5—v_6	30	0	0	21.523	2.176
v_3—v_6	30	0	0	21.52	1.142
v_5—v_7	30	0	0	21.522	4.330
v_6—v_8	30	0	0	21.521	1.626
v_8—v_{13}	30	0	0	21.522	2.951
v_7—v_8	30	0	0	21.522	1.768
v_9—v_{10}	12.556	29	2	20.661	1.098
v_{10}—v_{11}	30	0	0	21.526	0.772
v_{11}—v_{12}	30	0	0	20.522	1.881
v_{12}—v_{13}	30	0	0	20.522	1.281
v_{12}—v_{15}	30	0	0	20.523	4.210
v_{10}—v_{17}	30	0	0	20.523	1.368
v_{14}—v_{18}	30	0	0	20.512	1.624
v_{14}—v_{15}	30	0	0	20.512	3.490
v_{15}—v_{16}	30	0	0	20.517	1.254
v_7—v_{11}	30	0	0	20.523	1.211

Node 1 is at the center of the fire, and the path length objective function exerts a strong effect on the objective value F because of its far distance from Exit B. The optimal evacuation path planned for it by the bi-objective path planning model and algorithm is always v_1—v_4—v_5—v_6—v_3 with a path length of 47.6 m. The shortest evacuation path v_1—v_4—v_5—v_6—v_3 is determined to be the optimal evacuation path with an objective value F of 1.768 given that paths around Exit A are typically not disabled by the algorithm at 30 s of the fire. At 90 s of the fire, the risk level at node 1 is higher than that of other locations because this node is in the center of the fire. Paths around node 1 have generally reached the risk threshold, and people here face the situation of infeasible paths; hence, the algorithm restores forbidden paths and re-traverses them to obtain the path v_1—v_4—v_5—v_6—v_3 with the minimum objective value F, which is 2.688; The majority of locations in the building are filled with a high concentration of smoke and almost all paths have reached the risk threshold at 200 s of the fire. Therefore, the algorithm restores the forbidden paths, and the minimum path length v_1—v_4—v_5—v_6—v_3 with an objective value F of 2.772 is still determined to be the optimal evacuation path. The optimal evacuation path for node 1 is summarized in Table 12.

The optimal evacuation path for node 1 is different from the case of node 7, which is situated in the center of the building and far from the fire location. The optimal evacuation path of node 7 is determined via the crowding and path length

Table 9
Fire Data and Crowd Density for Each Path at 90 s of Fire

Path	Visibility (m)	CO (ppm)	HCN (ppm)	Temperature (°C)	Crowd Density (person/m^2)
v_1—v_4	1.186	325	23	50.168	1.934
v_4—v_5	1.342	281	19	43.09	2.372
v_4—v_{10}	0.803	486	34	54.231	1.032
v_2—v_5	1.626	224	15	32.102	0.430
v_5—v_6	3.3	109	8	27.727	2.126
v_3—v_6	2.096	165	13	29.694	0.303
v_5—v_7	2.302	157	11	29.495	1.050
v_6—v_8	5.469	65	4	24.345	0.344
v_8—v_{13}	26.14	14	1	21.712	0.542
v_7—v_8	26.483	13	1	21.710	0.516
v_9—v_{10}	0.812	466	32	44.908	1.358
v_{10}—v_{11}	2.38	152	11	29.824	0.049
v_{11}—v_{12}	8.427	42	3	23.683	1.940
v_{12}—v_{13}	7.37	48	3	23.107	0.313
v_{12}—v_{15}	5.14	69	5	24.212	0.086
v_{10}—v_{17}	0.593	653	45	51.071	1.376
v_{14}—v_{18}	30	0	0	21.093	0.368
v_{14}—v_{15}	30	0	0	21.093	1.145
v_{15}—v_{16}	30	0	0	20.159	0.645
v_7—v_{11}	5.497	65	4	26.963	1.646

when the smoke does not spread widely. The shortest evacuation path v_7—v_8—v_6—v_3 that avoids the congested path is optimal at 30 s. However, the fire risk objective function exerts a strong influence on the target value F as the fire progresses. The optimal evacuation path of node 7 at 90 and 200 s will no longer choose Exit A with a high risk level. Node 1 is located in the center of the fire and far from Exit B. Subject to the path length objective function, paths with extremely long lengths will be given high objective value and therefore will not be prioritized at three moments. The optimal evacuation path v_1—v_4—v_5—v_6—v_3 is always the path with the minimum objective value F.

4.3. Feasibility Analysis of Model Application

The application of the method in actual cases will be presented in this section. Detection data of the on-site path risk factor plays a decisive role in the accuracy of the calculation results of the model. CO concentration, HCN concentration, and visibility can be detected by fire smoke sensors; environment temperature in the path can be measured by temperature sensors; and crowd density in the path can be measured by IR camera when this model is applied to multi-exit buildings. The optimal evacuation path can be displayed in intelligent evacuation signs that can change the direction of indication in real time through the real-time calculation of path risk and length rather than being static similar to traditional evacuation signs that can direct escapees to a dangerous path.

Table 10
Fire Data and Crowd Density for Each Path at 200 s of Fire

Path	Visibility (m)	CO (ppm)	HCN (ppm)	Temperature (°C)	Crowd Density (person/m^2)
v_1—v_4	0.678	581	42	61.135	0.913
v_4—v_5	0.897	424	29	47.576	0.548
v_4—v_{10}	0.532	734	51	56.605	0.651
v_2—v_5	0.753	494	34	40.918	0.733
v_5—v_6	1.066	345	24	36.992	0.817
v_3—v_6	0.843	439	31	36.992	0.648
v_5—v_7	1.055	345	24	35.846	0.689
v_6—v_8	1.198	303	21	33.398	0.170
v_8—v_{13}	0.965	375	26	32.395	0.542
v_7—v_8	1.095	329	23	31.159	0.338
v_9—v_{10}	0.466	822	57	49.531	0.286
v_{10}—v_{11}	0.839	442	31	40.106	0.661
v_{11}—v_{12}	1.171	310	21	32.645	0.537
v_{12}—v_{13}	0.901	403	28	33.709	0.461
v_{12}—v_{15}	1.002	363	25	33.737	0.948
v_{10}—v_{17}	0.423	923	64	56.316	0.241
v_{14}—v_{18}	30	0	0	21.44	0.972
v_{14}—v_{15}	30	0	0	21.706	0.471
v_{15}—v_{16}	8.756	40	3	22.585	0.345
v_7—v_{11}	1.052	346	24	35.499	0.252

5. Discussion

5.1. *Meaning*

The length of evacuation path (which may result in additional evacuation time) as well as the harmful effect of fire on human health (which may lead to casualties) are considered in the proposed evacuation path decision model. Risk factors considered in this model are more comprehensive than most current models with fire risk as the optimization objective. Distinguishing from the way risk has been quantified in previous studies, a more homogeneous semiquantitative approach is used to quantify the effects of CO, HCN, temperature, visibility, and crowding on escapees. The risk index is calculated with reference to numerous previous studies to enhance the scientificity of the results. For example, AEGLs are used as a basis for quantifying CO and HCN.

Moreover, the modified Dijkstra algorithm improves not only the calculation efficiency in the case of multiple exits but also adjusts the weights of path length and risk in the optimal path. Compared with the conventional method that only sets risk thresholds for hazardous gases or temperatures, the modified Dijkstra algorithm does not initially consider the paths where CO, HCN, temperature, visibility, and congestion reach the risk threshold to ensure the safety of evacuation paths further. The model and method presented in this study will be useful for intelligent evacuation [42] in building fires and management of building fire safety.
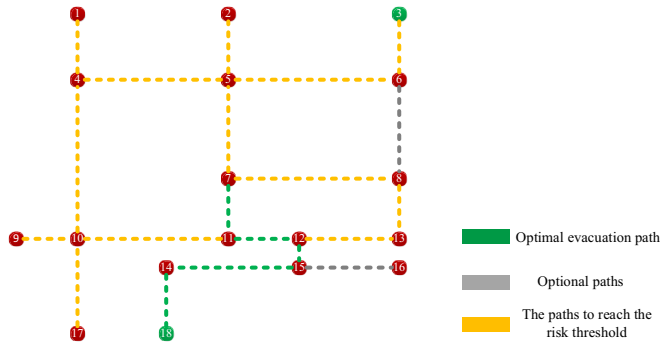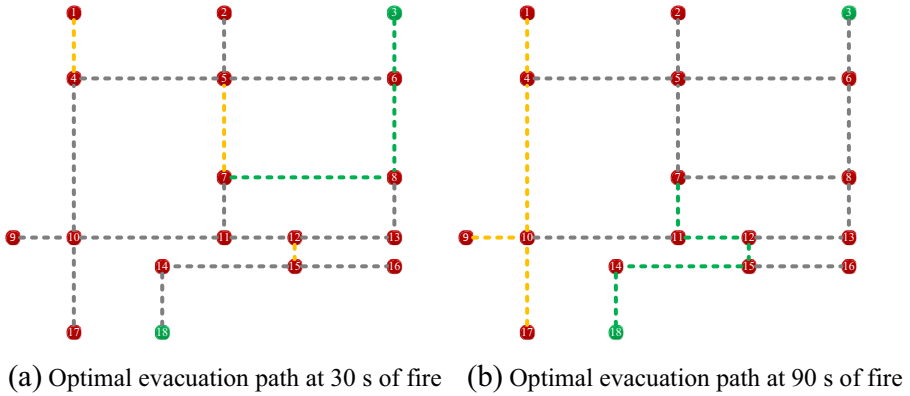
(a) Optimal evacuation path at 30 s of fire   (b) Optimal evacuation path at 90 s of fire

(c) Optimal evacuation path at 200 s of fire

Figure 6.   Optimal evacuation paths for node 7.

Table 11
Optimal Evacuation Path for Node 7

Node	Time	Optimal evacuation path	Objective value	Path length
v_7	30 s	v_7—v_8—v_6—v_3	0.035	34.7 m
	90 s	v_7—v_{11}—v_{12}—v_{15}—v_{14}—v_{18}	0.042	42.3 m
	200 s	v_7—v_{11}—v_{12}—v_{15}—v_{14}—v_{18}	1.302	42.3 m

5.2. Limitations

In this study, some necessary assumptions are given directly, whose credibility cannot be proven at present, but may be verified in the future.

(1) The grading standards are assumed directly in Table 1 (the risk index corre-
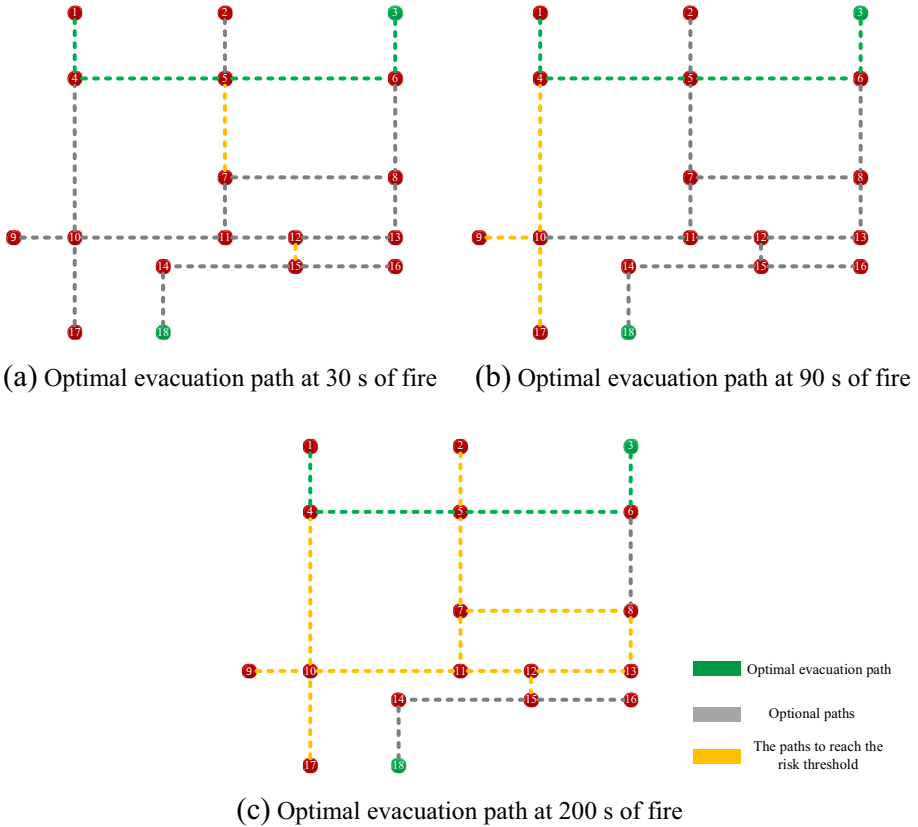sponding to each risk level is set to 0, 0.5, 0.7, and 1). Only four risk classifi-

(a) Optimal evacuation path at 30 s of fire

(b) Optimal evacuation path at 90 s of fire

(c) Optimal evacuation path at 200 s of fire

Figure 7. Optimal evacuation paths for node 1.

Table 12
Optimal Evacuation Path for Node 1

Node	Time	Optimal evacuation path	Objective value	Path length
v_1	30 s	$v_1—v_4—v_5—v_6—v_3$	1.768	47.6 m
	90 s	$v_1—v_4—v_5—v_6—v_3$	2.688	47.6 m
	200 s	$v_1—v_4—v_5—v_6—v_3$	2.772	47.6 m

cations exist, and the range of risk factor levels corresponding to each risk classification may be a wide range, such as a CO concentration of 150 and 400 ppm, both of which correspond to a risk index of 0.5. Future investigations may focus on working out a more detailed risk classification and narrowing the range of levels corresponding to each risk classification.

(2) The risk level corresponding to CO and HCN may be different from the actual situation, and the threshold of concentration may be small because

AEGLs are established on the basis of susceptible people who are more sensitive to harmful gases than the general population. Hence, the results may be conservative. Future investigations can focus on exploring the risk classification criteria for hazardous gases with high applicability to most populations.

(3) We set the weights of the five risk factors in the path risk level in the case study depending on how different risk factors affect evacuation and the degree of hazard to humans. For example, asphyxiating gases in fire, especially CO, present the maximum lethal risk factor and cause more than 50% of deaths due to asphyxiation (Statistics from Fire and Rescue Department Ministry of Emergency Management in China [43]). We therefore assigned a high weight to CO and HCN. However, our assumptions lack experimental basis. This supposition will be the premise of our future work to determine the weights of risk factors on the basis of a more scientific and rigorous approach.

6. Conclusion

A new decision method is proposed for generating optimal evacuation paths in real time. The method involves evacuation models that consider path length and risk and an optimization algorithm with dynamic adjustment capabilities.

The optimal evacuation path based on path length and risk considers risks, including CO concentration, HCN concentration, temperature, visibility, and crowding. A Semiquantitative approach was used to characterize the risk level of paths to improve the homogeneity of data. The modified Dijkstra algorithm was applied for optimization and the adjustment of the Pareto optimal solution of the two objectives as the fire progresses. The bi-objective model and algorithm directs pedestrians toward a safe path. The rationality and feasibility of the optimal evacuation path are verified using simulation experiment. The case analysis results showed that the optimal evacuation path obtained from the model can be adjusted with fire progression through the fire objective function.

The proposed method can plan an optimal path for evacuees of a multi-exit building fire in terms of combined path risk and length while ensuring safety and efficiency. However, this study neglected the physiological factors of people in fire events, such as falls, trips and walking speed. Moreover, a future investigation can focus on the validity of risk classification criteria in this study and risk factor weights as well as refining the case study methodology.

Acknowledgements

Declarations

Conflict of interest   We declare that we do not have any commercial or associative interest that represents a conflict of interest in connection with the work submitted.

References

1. Luo Y-x, Li Q, Jiang L-r, Zhou Y-h (2021) Analysis of Chinese fire statistics during the period 1997–2017. Fire Saf J 125:6–7
2. Lu S, Mei P, Wang J, Zhang H (2012) Fatality and influence factors in high-casualty fires: a correspondence analysis. Saf Sci 50(4):1019–1033. https://doi.org/10.1016/j.ssci.2011.12.006
3. Atec A, Hull R (2010) Fire Statistics. Woodhead Publishing Limited and CRC Press LLC, London
4. Pursals SC, Garzón FG (2009) Optimal building evacuation time considering evacuation routes. Eur J Oper Res 192(2):692–699. https://doi.org/10.1016/j.ejor.2007.10.004
5. Liu M, Zhang F, Ma Y, Pota HR, Shen W (2016) Evacuation path optimization based on quantum ant colony algorithm. Adv Eng Inform 30(3):259–267. https://doi.org/10.1016/j.aei.2016.04.005
6. Cuesta A, Abreu O, Balboa A, Alvear D (2017) Real-time evacuation route selection methodology for complex buildings. Fire Saf J 91:947–954. https://doi.org/10.1016/j.firesaf.2017.04.011
7. Li X, Li Q, Claramunt C (2018) A time-extended network model for staged evacuation planning. Saf Sci 108:225–236. https://doi.org/10.1016/j.ssci.2017.08.004
8. Aleksandrov M, Cheng C, Rajabifard A, Kalantari M (2019) Modelling and finding optimal evacuation strategy for tall buildings. Saf Sci 115:247–255. https://doi.org/10.1016/j.ssci.2019.02.017
9. Gao H, Medjdoub B, Luo H, Zhong H, Zhong B, Sheng D (2020) Building evacuation time optimization using constraint-based design approach. Sustain Cities Soc 9:7–8
10. Cao Y, Luo C, Liu Y, Teng S, Xin G (2021) Path intelligent optimization for dense crowd emergency evacuation in heritage buildings. J Cult Herit 47:180–187. https://doi.org/10.1016/j.culher.2020.06.007
11. Kurdi H, Almulifi A, Al-Megren S, Youcef-Toumi K (2021) A balanced evacuation algorithm for facilities with multiple exits. Eur J Oper Res 289(1):285–296. https://doi.org/10.1016/j.ejor.2020.07.012
12. Miñambres MD, Llanos DR, Gento AM (2022) Extending and validating a theoretical model to predict the effectiveness of building evacuations. J Build Eng . https://doi.org/10.1016/j.jobe.2022.104256
13. von Schantz A, Ehtamo H (2022) Minimizing the evacuation time of a crowd from a complex building using rescue guides. Phys A: Stat Mech Appl . https://doi.org/10.1016/j.physa.2022.127011
14. Balboa A, González-Villa J, Cuesta A, Abreu O, Alvear D (2020) Testing a real-time intelligent evacuation guiding system for complex buildings. Saf Sci . https://doi.org/10.1016/j.ssci.2020.104970
15. Wang J, Yu X, Zong R, Lu S (2022) Evacuation route optimization under real-time toxic gas dispersion through CFD simulation and Dijkstra algorithm. J Loss Prev Process Ind . https://doi.org/10.1016/j.jlp.2022.104733

16. Faouzi Kamouna MEB (2021) Fatna Belqasmic, Abderrazak Hachania A smart dynamic crowd evacuation system for exhibition centers. Procedia Comput Sci 184:218–225

17. Wang Y, Ma W, Wang T, Liu J, Wang X, Sean M et al (2022) Dynamic optimisation of evacuation route in the fire scenarios of offshore drilling platforms. Ocean Eng . https://doi.org/10.1016/j.oceaneng.2022.110564

18. Chu JC, Chen AY, Lin Y-F (2017) Variable guidance for pedestrian evacuation considering congestion, hazard, and compliance behavior. Transp Res Part C Emerg Technol 85:664–683. https://doi.org/10.1016/j.trc.2017.10.009

19. Mirahadi F, McCabe BY (2021) EvacuSafe: a real-time model for building evacuation based on Dijkstra's algorithm. J Build Eng . https://doi.org/10.1016/j.jobe.2020.101687

20. Song Y, Niu L, Liu P, Li Y (2021) Fire hazard assessment with indoor spaces for evacuation route selection in building fire scenarios. Indoor Built Environ 31(2):452–465. https://doi.org/10.1177/1420326x21997547

21. Shi X, Gai W, Xu K (2022) Bi-objective rescue path selection optimization for mine fires based on quantitative risk assessment. Saf Sci . https://doi.org/10.1016/j.ssci.2021.105492

22. He Z, Liu C, Chu X, Negenborn RR, Wu Q (2022) Dynamic anti-collision A-star algorithm for multi-ship encounter situations. Appl Ocean Res . https://doi.org/10.1016/j.apor.2021.102995

23. Ikeda Y, Inoue M (2016) An Evacuation route planning for safety route guidance system after natural disaster using multi-objective genetic algorithm. Procedia Comput Sci 96:1323–1331. https://doi.org/10.1016/j.procs.2016.08.177

24. Samany NN, Sheybani M, Zlatanova S (2021) Detection of safe areas in flood as emergency evacuation stations using modified particle swarm optimization with local search. Appl Soft Comput . https://doi.org/10.1016/j.asoc.2021.107681

25. Liu H, Xu B, Lu D, Zhang G (2018) A path planning approach for crowd evacuation in buildings based on improved artificial bee colony algorithm. Appl Soft Comput 68:360–376. https://doi.org/10.1016/j.asoc.2018.04.015

26. Contreras-Cruz MA, Ayala-Ramirez V, Hernandez-Belmonte UH (2015) Mobile robot path planning using artificial bee colony and evolutionary programming. Appl Soft Comput 30:319–328. https://doi.org/10.1016/j.asoc.2015.01.067

27. Wang H, Mao W, Eriksson L (2019) A Three-dimensional dijkstra's algorithm for multi-objective ship voyage optimization. Ocean Eng . https://doi.org/10.1016/j.oceaneng.2019.106131

28. Biyela P, Rawatlal R (2019) Development of an optimal state transition graph for trajectory optimisation of dynamic systems by application of Dijkstra's algorithm. Comput Chem Eng 125:569–586. https://doi.org/10.1016/j.compchemeng.2019.03.025

29. Fink W, Baker VR, Brooks AJW, Flammia M, Dohm JM, Tarbell MA (2019) Globally optimal rover traverse planning in 3D using Dijkstra's algorithm for multi-objective deployment scenarios. Planet Space Sci . https://doi.org/10.1016/j.pss.2019.104707

30. Shukla DK, Arul AJ (2021) An efficient Dijkstra's semaphore based k-out-of-n Petri net voting model: An application to shutdown actuation system reliability. Ann Nucl Energy . https://doi.org/10.1016/j.anucene.2021.108218

31. Kim D, Kim D, Woo D, Lee Y (2022) Development of an image analysis code for hydrided Zircaloy using Dijkstra's algorithm and sensitivity analysis of radial hydride continuous path. J Nucl Mater 564:3–5. https://doi.org/10.1016/j.jnucmat.2022.153647

32. Zhou Y, Huang N (2022) Airport AGV path optimization model based on ant colony algorithm to optimize Dijkstra algorithm in urban systems. Sustain Comput: Inform Syst . https://doi.org/10.1016/j.suscom.2022.100716

33. Yuan Y, Wang D (2009) Path selection model and algorithm for emergency logistics management. Comput Ind Eng 56(3):1081–1094. https://doi.org/10.1016/j.cie.2008.09.033
34. Zhang J, Zhao J, Song Z, Gao J (2020) Evacuation performance of participants in an offshore platform under smoke situations. Ocean Eng . https://doi.org/10.1016/j.oceaneng.2020.107739
35. Huo F, Li Y, Li C, Ma Y (2022) An extended model describing pedestrian evacuation considering pedestrian crowding and stampede behavior. Physica A . https://doi.org/10.1016/j.physa.2022.127907
36. NRC (2010) Acute Exposure Guideline Levels for Selected Airborne Chemicals:, 8National Academies Press (US), Washington
37. NRC (2002) Acute Exposure Guideline Levels for Selected Airborne Chemicals:, 2National Academies Press (US), Washington
38. Casey C. Grant PE, John R. HallJr. PD, Robert E. Solomon PE (2008) NFPA-Fire Protection Handbook-2008–20th. National Fire Protection Association, Quincy, Massachusetts
39. Ibrahim AM, Venkat I, Subramanian KG, Khader AT, Wilde PD (2016) Intelligent evacuation management systems. ACM Trans Intell Syst Technol 7(3):1–27. https://doi.org/10.1145/2842630
40. Xu K, Gai W-m, Salhi S (2021) Dynamic emergency route planning for major chemical accidents: Models and application. Saf Sci . https://doi.org/10.1016/j.ssci.2020.105113
41. García-Ojeda JC, Bertok B, Friedler F, Fan LT (2013) Building-evacuation-route planning via time-expanded process-network synthesis. Fire Saf J 61:338–347. https://doi.org/10.1016/j.firesaf.2013.09.023
42. Balboa A, González-Villa J, Cuesta A, Abreu O, Alvear D (2020) Testing a real-time intelligent evacuation guiding system for complex buildings. Saf Sci 132:104970–104972
43. National Fire and Rescue Administration (China). Nearly ten years 35 group deaths and injuries in fires killed 677 people, these reasons caused such a major casualty. 2020. Available from: https ://www.119.gov.cn/gk/sjtj/2022/1337.shtml